

Iron nanoparticles green-formulated by *Coriandrum sativum* leaf aqueous extract: investigation of its anti-liver-cancer effects

Qianli Zhan¹, Jing Han², Liting Sheng¹

¹Department of General Practice, Baoding No. 1 Central Hospital, Baoding City, Hebei Province, China

²Department of Gastroenterology, Baoding No. 1 Central Hospital, Baoding City, Hebei Province, China

Submitted: 30 August 2021; **Accepted:** 7 December 2021

Online publication: 14 December 2021

Arch Med Sci

DOI: <https://doi.org/10.5114/aoms/144627>

Copyright © 2022 Termedia & Banach

Corresponding author:

Jing Han

Department

of Gastroenterology

Baoding No. 1 Central Hospital

320, Great Wall North Street

Baoding City

Hebei Province, China

E-mail: hanjing0618@126.com

com

Abstract

Introduction: An eco-friendly biosynthesized FeNP immobilized *Coriandrum sativum* extract has been introduced.

Material and methods: The as-prepared nanoparticles (FeNPs) were characterized using UV-Vis, SEM, and FT-IR. It was shown that the iron nanoparticles have spherical shape and uniform size.

Results: The synthesized nanoparticles have very low cell viability and high anti-liver cancer activities dose-dependently against pleomorphic hepatocellular carcinoma (SNU-387), hepatic ductal carcinoma (LMH/2A), Morris hepatoma (McA-RH7777), and Novikoff hepatoma (N1-S1 Fudr) cell lines without any cytotoxicity on the normal cell line (HUVEC). The synthesized nanoparticles inhibited half of the DPPH molecules in the concentration of 132 µg/ml. Perhaps notable anti-liver cancer activities of the synthesized nanoparticles against common liver cancer cell lines are linked to their antioxidant activities.

Conclusions: Our results show that the FeNPs from *Coriandrum sativum* extract are apposite stabilizing agents, which serve as an effective anticancer agent against liver cancer cell lines.

Key words: iron nanoparticles, *Coriandrum sativum* extract, liver cancer, antioxidant.

Introduction

Liver is an essential organ accountable for the metabolism, bile secretion, elimination of many substances, blood detoxifications, and synthesis and regulation of vital hormones [1]. Liver diseases have proven to be a global problem and are associated with substantial morbidity and mortality [2]. The main contributory factors for liver diseases in developed countries are alcohol consumption and viral-induced chronic liver diseases, while in developing countries the most common causes are environmental toxins, (carbon tetrachloride (CCl₄) and insecticides), hepatitis B and C viruses, and hepatotoxic drugs (certain antibiotics, chemotherapeutic agents, high doses of paracetamol, etc.) [1, 2]. Chronic liver cirrhosis and drug-induced liver injury comprise the ninth leading cause of death in western and developing countries [1]. Among all liver

diseases, liver cancers are the most deadly. Liver cancer or hepatic cancer first occurs in the liver, and after progression of the disease it transfers to all parts of the body via the lymphatic system or bloodstream [2]. The main types of hepatic cancers are hepatobiliary cancers, hepatocellular carcinoma, cholangiocarcinoma, liver angiosarcoma, and hepatoblastoma. Among all hepatic cancers, the role of hepatobiliary cancers in the death of humans is significant. Hepatobiliary cancers are divided to several types, including extrahepatic cholangiocarcinoma, intrahepatic cholangiocarcinoma, gallbladder cancer, and hepatobiliary carcinoma [2]. The common risk factors of hepatobiliary carcinoma are external sources, particular conditions or comorbidities, and infection with the hepatitis C (HCV) and/or B (HBV) virus [3]. The main symptoms of hepatobiliary carcinoma are nonspecific (upper abdominal pain, malaise, weight loss, anorexia, and jaundice), physical (ascites and hepatomegaly), and paraneoplastic (hypoglycaemia, hypercalcaemia, erythrocytosis, and hypercholesterolaemia) [4]. Medical history and physical examination, molecular testing, sputum cytology, blood tests, thoracentesis, needle biopsy, and medical imaging such as positron emission tomography, magnetic resonance imaging, low-dose helical computerized tomography scan, computerized tomography, and chest X-ray are used for the diagnosis of hepatobiliary carcinoma [5]. For the treatment of hepatobiliary carcinoma, surgery, radiation therapy, chemotherapy, targeted therapy, immunotherapy, and EGFR-targeted therapy are used [4, 5]. The main anti-hepatobiliary carcinoma chemotherapeutic drugs include cisplatin with lipiodol, sorafenib, and doxorubicin [2]. According to the side effects of chemotherapeutic drugs, such as mouth sores, weight loss, diarrhoea, vomiting, hair loss, fatigue, and nausea, the formulation of modern chemotherapeutic drugs is necessary [6]. Recently, scientists have understood that metallic nanoparticles, especially iron nanoparticles, have excellent anticancer properties [7].

Various pathways have been developed for the biogenic or biological formulation of nanomaterials from the salts of different metal ions. The synthesis of nanoparticles under purely 'green' principles can be achieved by using an environmentally compatible solvent system with environmentally-friendly stabilizing and reducing factors [8–12]. The basic principle in the biogenesis of nanoparticles is reduction of metal ions of several biomolecules found in vital organisms. In addition to reducing the environmental impact of biological synthesis, this critical step enables the production of large quantities of nanoparticles, which are well-defined in size and morphology, and independent of contamination. Microorganisms, marine algae, plant

extracts, plant tissue, fruits, and all plants are used to formulate nanomaterials [10–13].

Recently, scientists have revealed that medicinal plants' green synthesized-metallic nanoparticles possess excellent anti-cancer properties. In fact, the green synthesized metallic nanoparticles have achieved notable consideration in a variety of medicinal disciplines [9–12]. Some relevant conducted studies have shown that some nanoparticles (especially platinum, gold, and silver nanoparticles) have promising therapeutic properties, accounting for their potential use as excellent alternatives to physiochemically different metal-supported nanoparticles, antibacterial, and particularly anticancer drugs (such as cisplatin and azathioprine) [10–17].

Previous studies have indicated the anticancer effects of metallic nanoparticles against various cell lines such as Lewis lung carcinoma (LL2) cells, ADR/MCF-7 cancer cells, A549 lung epithelial cancer cell line, HT29, HCT15, HCT116, and RKO colon cancer cell lines, U87 and LN229 human glioma cancer lines, A549 cells and HeLa cells, HepG2-R, HDF together with C0045C, 4T1 mouse mammary carcinoma, and A549, H460, and H520 human lung cancer cells [11–13]. A brief survey of the literature demonstrates that no study has been performed on the remedial capacities of natural compound green-synthesized metallic nanoparticles in treating liver cancer so far. In a study, a co-treatment of sodium nitroprusside and 5-fluorouracil resulted in inhibition of the cytotoxic effect of 5-fluorouracil, while a combination treatment of nickel nanoparticles with Na_2S , sodium nitroprusside, and 5-fluorouracil caused highly significant cytotoxicity against colorectal cancer cell lines. Direct sequencing reveals new mutations, mainly of intronic variation in the endothelial NO synthase gene, which has not previously been described in the database. These findings indicate that H_2S promotes the anticancer efficiency of 5-fluorouracil in the presence of nickel nanoparticles, while NO has antiapoptotic activity in colorectal cancer cell lines [16, 17]. A study by Chen *et al.* revealed the anti-immortalized myelogenous leukaemia activities of metallic nanoparticles green-synthesized by the *Tsoong* herb against K562 cell line under *in vitro* conditions. In addition, the previous metallic nanoparticles treated leukaemic mice for less than 20 days [14]. In the study of Rameshthangam and Pandian Chitra, leaf extract of the medicinally important plant *Ocimum sanctum* (*O. sanctum*) has been used to synthesize the metallic nanoparticles and extraction of quercetin. Quercetin has been conjugated with nickel nanoparticles for an enhanced anticancer effect on human breast cancer MCF-7 cells. Extracted quercetin was conjugated with polyethylene glycol-coated nickel nanoparticles (quercetin–polyethylene gly-

col-nickel nanoparticles) used as carriers for breast cancer treatment. Anticancer activity of quercetin-polyethylene glycol-nickel nanoparticles was evaluated by assessing cell viability, reactive oxygen species (ROS) production, caspase activity, mitochondrial membrane potential (MMP), and changes in nuclear morphology (staining methods) [15].

The present experiment was conducted to evaluate the possible anti-liver cancer activity of synthesized iron nanoparticles using an aqueous extract prepared from the leaves of *Coriandrum sativum* against common cell lines of liver cancer including pleomorphic hepatocellular carcinoma (SNU-387), hepatic ductal carcinoma (LMH/2A), Morris hepatoma (McA-RH7777), and Novikoff hepatoma (N1-S1 Fudr).

Material and methods

Material

Bovine serum, 2,2-diphenyl-1-picrylhydrazyl (DPPH), dimethyl sulfoxide (DMSO), decampmaneh foetal, 4-(dimethylamino) benzaldehyde, hydrolyzate, antimycotic antibiotic solution, Ehrlich solution, and borax-sulfuric acid mixture, DMED, all were afforded from the US Sigma-Aldrich company.

Preparation and extraction of the aqueous extract of *Coriandrum sativum* leaf

To obtain the aqueous extract of the plant, 250 g portions of the dried branches of the *Coriandrum sativum* leaves were poured into a container containing 2000 ml boiled water, and the container lid was tightly closed for 4 h. Then, the content of the container was filtered, and the remaining liquid was placed on a bain-marie to evaporate. Finally, a tar-like material was obtained, which was powdered using a freeze dryer.

Preparation and optimization of FeNP synthesis

A 10 ml aqueous extract solution (20 mg/ml) was added to 30 ml of $\text{FeCl}_3 \times 6 \text{H}_2\text{O}$ in a concentration of 0.02 M (deionized water was used for all steps of this section). The mixture was refluxed for 90 min at 50°C. A colour change from yellow to black indicated the formation of iron nanoparticles. The precipitate was triple washed with water and subsequently centrifuged at 12,000 rpm for 15 min. The obtained black powder was kept in a vial for the chemical characterization and evaluation of its biological activity.

Chemical characterization techniques

UV-Vis and FT-IR spectroscopy and SEM techniques were used to characterize the biosyn-

thesized FeNPs. Different parameters of the nanoparticles, such as shape, particle size, fractal dimensions, crystallinity, and surface area, were evaluated by these techniques. The FT-IR spectra were recorded using a Shimadzu FT-IR 8400 in the range 400–4000 cm^{-1} (KBr disc), while MIRA3TESCAN-XMU was used to report the FE-SEM images.

Measurement of cell toxicity of FeNPs

In the present study, the anti-human liver cancer and cytotoxicity potentials of $\text{NiSO}_4 \times 6 \text{H}_2\text{O}$, *Coriandrum sativum* leaf aqueous extract, and FeNPs were assessed by MTT assay against normal (HUVEC) and liver cancer (pleomorphic hepatocellular carcinoma (SNU-387), hepatic ductal carcinoma (LMH/2A), Morris hepatoma (McA-RH7777), and Novikoff hepatoma (N1-S1 Fudr)) cell lines under *in vitro* conditions. They were then cultured as a monolayer culture in 90% RPMI-1640 medium and 10% foetal serum and were immediately supplemented with 200 mg/ml streptomycin, 125 mg/ml penicillin, and 8 mg/ml amphotericin B. The culture was then exposed to 0.5 atm carbon dioxide at 37°C, and the tests were performed after at least 10 successful passages. MTT is an assay used to investigate the toxic effects of various materials on various cell lines, including non-cancer and cancer cells. To evaluate the cell toxicity effects of the compounds used in this research, the cells were transferred from the T25 flask to the 96-well flasks. In each cell of the 96-cell flasks, 7000 cells of cancer and fibroblast cell lines were cultured, and the volume of each cell was eventually increased to 100 μl . Before treating the cells in the 96-well flasks, the density of cells was increased to 70%, so the 96-well flasks were incubated for 24 h to obtain the cell density of 7×10^3 . Thereafter, the initial culture medium was discarded, and variable concentrations (0–1000 $\mu\text{g/ml}$) of $\text{NiSO}_4 \times 6 \text{H}_2\text{O}$, *Coriandrum sativum* leaf aqueous extract, and FeNPs were incubated at 37°C and 5% CO_2 for 24, 48, and 72 h. Then, 20 μl MTT was added to each well. This step was followed by the addition of 100 μl of DMSO solvent to each well. The treated wells were then kept at room temperature for 25 min and read at 490 and 630 nm by a 1 μl plate reader. The cell lines were also treated with hydroalcoholic extract (1.25 mg/ml), which inhibited about 20% of the cell growth. The annexin/PI method was used to determine the apoptosis level in the treated and control cell lines using a flow cytometry machine. Under optimized experimental conditions, the cell lines were treated with variable concentrations (0–1000 $\mu\text{g/ml}$) of $\text{NiSO}_4 \cdot 6\text{H}_2\text{O}$, *Coriandrum sativum* leaf aqueous extract, and FeNPs for 24 h. Cells were irrigated with phosphate-buffered saline (PBS). After centrifugation, buffer binding was added to the

obtained precipitate. Then, 5 μl annexin V dye was added and incubated for 15 min at 25°C. Cells were washed with the binding solution, followed by the addition of 10 μl of PI dye. Finally, cell analysis was conducted by a flow cytometry machine according to the following formula [18, 19]: Cell viability (%) = (sample A/Control A) \times 100.

Investigation of the antioxidant capacity of FeNPs

To determine the radical scavenging activity of the $\text{NiSO}_4 \times 6 \text{H}_2\text{O}$, *Coriandrum sativum* leaf aqueous extract, and FeNPs, 1 ml of 50 μM DPPH was combined with 1 ml of variable concentrations (0–1000 $\mu\text{g}/\text{ml}$) of $\text{NiSO}_4 \times 6 \text{H}_2\text{O}$, *Coriandrum sativum* leaf aqueous extract, and FeNPs. Then, they were mixed at 37°C for 1 h. The absorption rate of the samples was determined at 520 nm by a spectrophotometer, and the antioxidant activity was calculated using the following formula [20]: Inhibition (%) = (Sample A/Control A) \times 100.

The blank sample contained 1 ml methanol and 1 ml $\text{NiSO}_4 \cdot 6\text{H}_2\text{O}$, *Coriandrum sativum* leaf aqueous extract, and FeNPs, and a sample of 1 ml DPPH and 2 ml $\text{NiSO}_4 \times 6 \text{H}_2\text{O}$, *Coriandrum sativum* leaf aqueous extract, and FeNPs with the applied concentrations was used as a negative control.

Calculation of the half-maximal inhibitory concentration (IC_{50}) is a suitable method for comprising the activity of pharmaceutical-based materials. In this method, the measurement and comparison criterion is the concentration in which 50% of the final activity of the drug occurs. In this experiment, the IC_{50} of various repeats is estimated and compared with the IC_{50} of BHT, which is introduced as the antioxidant activity index. The closer the obtained value to the IC_{50} of BHT, the stronger the antioxidant activity of the material. The graph of the IC_{50} of the extract was produced by drawing the percentage inhibition curve against the extract concentration. First, 3 stock samples with variable

concentrations (0–1000 $\mu\text{g}/\text{ml}$) of $\text{NiSO}_4 \times 6 \text{H}_2\text{O}$, *Coriandrum sativum* leaf aqueous extract, and FeNPs were prepared. Then, a serial dilution was prepared from each sample, and the IC_{50} of the above samples was measured separately. Finally their mean was calculated. BHT, with different concentrations, was considered as a positive control. All experiments were performed in triplicate.

Statistical analysis

The obtained results were analysed by SPSS (version 20) software using one-way ANOVA, followed by Duncan post hoc test ($p \leq 0.01$).

Results and Discussion

Characterization of FeNPs

The UV-Vis spectra of biosynthesized FeNPs using the aqueous extract of *Coriandrum sativum* are shown in Figure 1. The surface plasmon resonance of FeNPs was confirmed by UV-Vis and compared with a previous report; the appearance of a band at the wavelength of 288 nm confirmed the formation of FeNPs [21].

In the FT-IR spectrum of metal oxides, the vibration band for the metal-oxygen bond usually appears in 400 to 700 cm^{-1} . Figure 2 presents the spectra of FeNPs. The peaks at 471, 526, and 611 cm^{-1} are attributed to the bending vibration of Fe-O. These peaks for iron oxide nanoparticles have been reported previously with a small difference in the respective wavenumber [22–24]. FT-IR spectroscopy is a reliable strategy to evaluate the plant's secondary metabolites because the capping and reducing agents of iron are precursors to FeNPs. According to the findings of this report, the FT-IR spectra of FeNPs and *Coriandrum sativum* extract were very similar to each other, confirming the successful biosynthesis of the iron nanoparticles. The presence of different IR bands correlates with the existence of various functional groups in

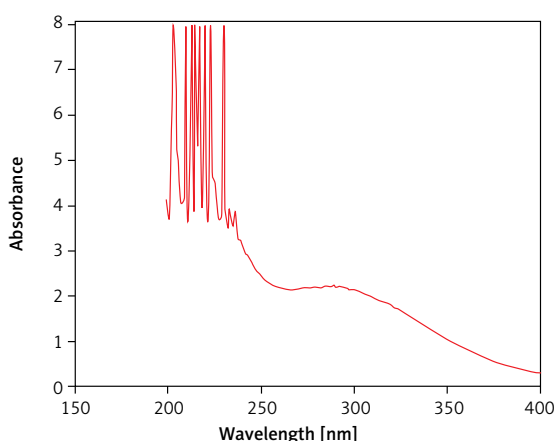


Figure 1. UV-Vis spectrum of biosynthesized FeNPs

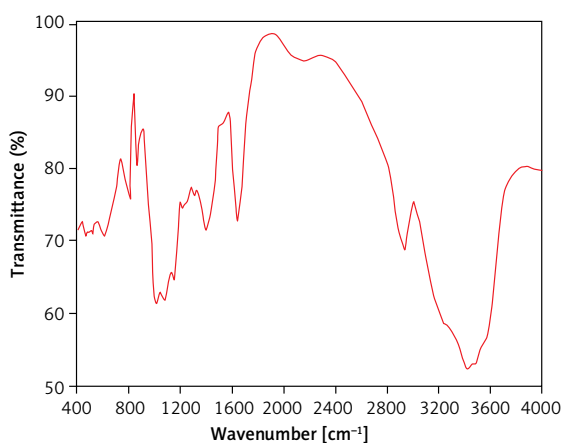


Figure 2. FT-IR spectrum of FeNPs and *Coriandrum sativum* extract

Coriandrum sativum extract. For instance, peaks at 3419 and 2932 cm^{-1} are related to O-H and aliphatic C-H stretching; peaks at a range of 1402 to 1631 cm^{-1} correspond to C=C and C=O stretching, while a peak at 1026 cm^{-1} could be ascribed to C-O stretching. These peaks can be generally considered to confirm the presence of various valuable natural compounds such as phenolic, flavonoid, saponins, quinones, and terpenoids, which have been reported previously in a number of plant extracts [25–27]. In the biosynthesis process of metallic nanoparticles, the secondary metabolites of plant extracts, as reducing, stabilizing, and dispersing agents, usually bind to NPs through their functional groups of hydroxyl and carbonyl [28–30].

The SEM images of FeNPs shown in Figure 3 depict a spherical morphology for the prepared FeNPs reported previously [31]. The figure also confirms the uniformity, good dispersion, and homogeneity of the FeNPs. Like the other metallic nanoparticles being synthesized using green chemistry approaches, a tendency to aggregate is observed for FeNPs. This property has been reported for other types of biosynthesized nanoparticles, i.e. FeNPs, ZnNPs, AgNPs, MnNPs, and SnNPs [29, 32–36]. On average, the diameter of the particle size for FeNPs was 21.43 nm.

Antioxidant properties of FeNPs against DPPH

In the present study, the DPPH free-radical scavenging potential of *Coriandrum sativum* leaf aqueous extract and FeNPs in a wide range of concentrations revealed impressive prevention, similar to that of BHT as a standard antioxidant agent. Free radicals are molecules that do not have a complete electron shell and are capable of increasing the chemical reaction compared to others. They are formed if the human body is exposed to tobacco smoke or radiation. In humans, the most important free radical is oxygen. When an oxygen molecule (O_2) is exposed to radiation, it removes an electron from the other molecules, destroying DNA and other molecules. Some of these changes may cause a number of persistent diseases, e.g. heart problems, muscle failure, diabetes, and cancer [20]. Antioxidants act like a broom against free radicals and have been recognized as powerful remedies to destroy free radicals and regenerate the damaged cells. More importantly, laboratory evidence has shown that antioxidants can effectively prevent cancer [13–16]. The IC_{50} of BHT and FeNPs were 91 and 132 $\mu\text{g}/\text{ml}$, respectively (Figure 4; Table I).

Metallic nanoparticles also have excellent potential to inhibit DPPH. The results obtained in our study are in line with many studies in which the mutual effect was monitored to increase the an-

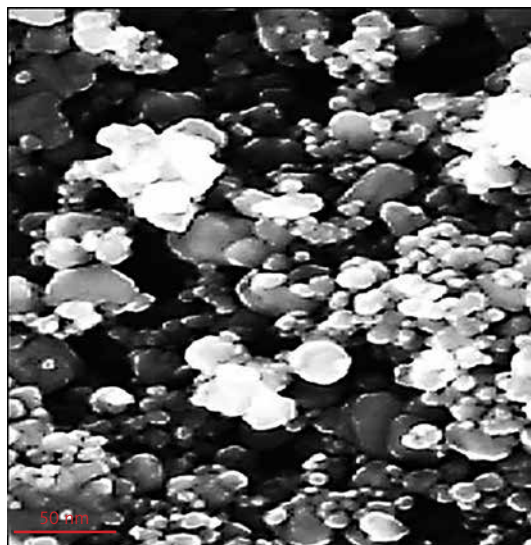


Figure 3. FE-SEM image of FeNPs

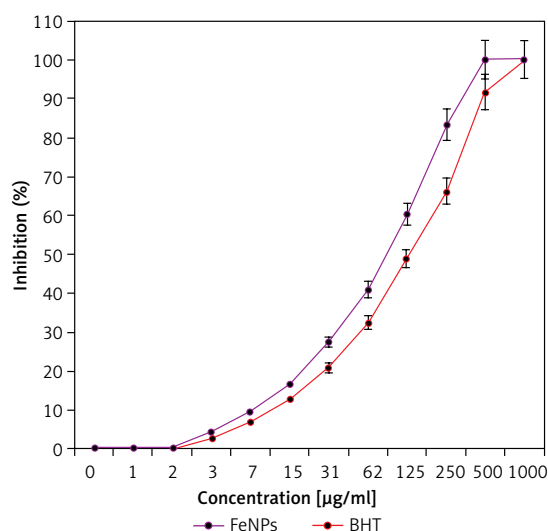


Figure 4. The antioxidant properties of FeNPs and BHT against DPPH

Table I. The IC_{50} of FeNPs and BHT in antioxidant test

| | FeNPs [$\mu\text{g}/\text{ml}$] | BHT [$\mu\text{g}/\text{ml}$] |
|-------------------------------|-----------------------------------|---------------------------------|
| IC_{50} against DPPH | 132 | 91 |

tiioxidant capacities between herbs and metallic salts against DPPH [13–16].

In general, metallic nanoparticles display remarkable and extraordinary antioxidant impacts, among which the antioxidant effects of FeNPs have been well documented. When FeNPs are synthesized with medicinal plants, the iron element forms a very strong bond with flavonoid and phenolic compounds, creating unique antioxidant effects. In a previous study, it was indicated that *Coriandrum sativum* is a rich source of antioxidant compounds, including terpenoid compounds, which were previously mentioned. It is also note-

Table II. The IC50 of FeNPs in the anti-liver cancer tests

| Cells | FeNPs [$\mu\text{g/ml}$] | |
|--------------------|----------------------------|-----|
| Liver cancer cells | N1-S1 Fudr | 200 |
| | McA-RH7777 | 225 |
| | LMH/2A | 159 |
| | SNU-387 | 180 |

worthy that the excellent antioxidant properties of *Coriandrum sativum* leaf aqueous extract can be attributed to the presence of these valuable natural compounds [17]. Several studies were carried out in the nanotechnology field using various medicinal plants, but to the best of our knowledge, no report is available on FeNPs synthesized using *Coriandrum sativum* leaf aqueous extract.

Many researchers have reported that FeNPs synthesized by ethnomedicinal plants with high antioxidant compounds play a remarkable role in removing free radicals and growth inhibition of all cancerous cells [37–40].

Most probably the significant anti-colon cancer potential of FeNPs synthesized by *Coriandrum sativum* aqueous extract against liver cancer cell lines is linked to their antioxidant activities. Similar studies have revealed that antioxidant materials such as metallic nanoparticles especially FeNPs and eth-

nomedicinal plants reduce the volume of tumours by removing free radicals [37]. The high presence of free radicals in the normal cells causes many mutations in their DNA and RNA, destroying their gene expression, and then accelerating the proliferation and growth of abnormal or cancerous cells.

The prevalence of free radicals in different types of cancer, such as skin, throat, ovarian, testicular, bladder, colon, small intestine, gastrointestinal stromal, stomach, breast, lung, vaginal, prostate, pancreatic, liver, gallbladder, hypopharyngeal, fallopian tube, thyroid, oesophageal, parathyroid, bile duct, and rectal cancers, indicates the significant role of these molecules in making angiogenesis and tumourigenesis [38, 39].

Cytotoxicity potential of FeNPs nanoparticles

In our study, the treated cells with several concentrations of the present iron salt, *Coriandrum sativum*, and FeNPs were examined by MTT test for 48 h to assess the cytotoxicity properties on normal (HUVEC) and liver cancer (pleomorphic hepatocellular carcinoma (SNU-387), hepatic ductal carcinoma (LMH/2A), Morris hepatoma (McA-RH7777), and Novikoff hepatoma (N1-S1 Fudr)) cell lines (Tables II, Figure 5). The absorbance was read at 570 nm, which indicated extraordinary viability

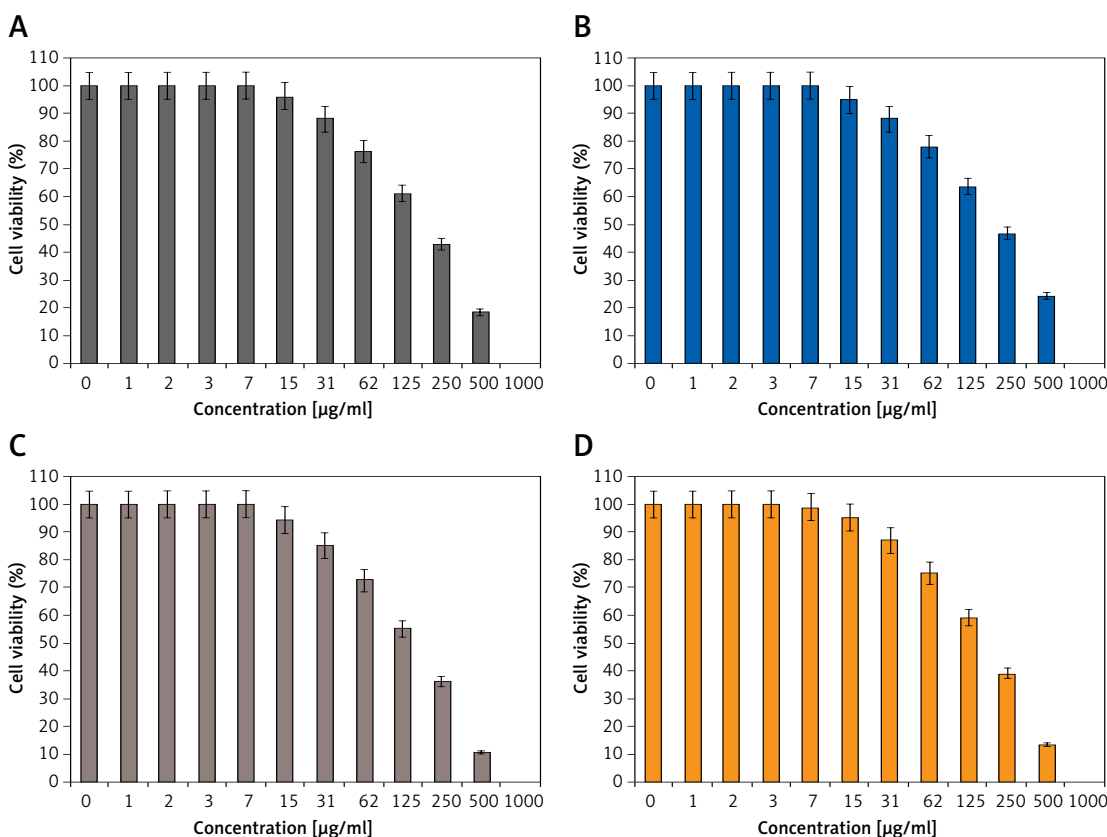


Figure 5. The anti-liver cancer properties of FeNPs against N1-S1 Fudr (A), McA-RH7777 (B), LMH/2A (C), and SNU-387 (D) cell lines

on normal cell line (HUVEC), even up to 1000 µg/ml, for iron salt, *Coriandrum sativum*, and FeNPs.

In colon cancer cell lines, their viability decreased dose-dependently in the presence of iron salt, *Coriandrum sativum*, and FeNPs. A simple perusal of the obtained results demonstrates that the best IC₅₀ of cytotoxicity property of FeNPs was seen in the case of the LMH/2A cell line against the above-used cell lines.

Among the various agents of metallic nanoparticles, such as surface functions nature, texture, size, and morphology, the size efficacy is of prime significance in the anticancer tests. In this context, previous reports have shown that the anticancer property is enhanced with a reduction in size of particle, based on their better penetration properties through the cell lines. Moreover, it has been determined that the size of particle lower than 100 nm demonstrates a better effect in the corresponding cancer cell lines [38–40]. As shown in Figure 3 of the present study, the sizes of iron nanoparticles biosynthesized by *Coriandrum sativum* leaf aqueous extract is at the average size of 21.43 nm.

In conclusion, in this research, to evaluate the main characteristics of the synthesized nanoparticles, FE-SEM, UV-Vis, and FT-IR methods were utilized, and the relevant results revealed that iron nanoparticles had been successfully synthesized. In the FE-SEM technique, the mean size of iron nanoparticles was assessed to be 21.43 nm, which is favourable. Bases on the FT-IR spectrum, the presence of a great number of antioxidant compounds produced appropriate conditions for reducing iron. On the other hand, the iron nanoparticles showed the best antioxidant activities against DPPH. Iron nanoparticles had appropriate anti-liver cancer activities dose-dependently against liver cancer (pleomorphic hepatocellular carcinoma (SNU-387), hepatic ductal carcinoma (LMH/2A), Morris hepatoma (McA-RH7777), and Novikoff hepatoma (N1-S1 Fudr)) cell lines without any cytotoxicity on the normal cell line (HUVEC).

Acknowledgments

Qian-li Zhan and Jing Han contributed equally to the work.

Conflict of interest

The authors declare no conflict of interest.

References

- Hodgson E, Smart RC. Introduction to Biochemical Toxicology. 3rd ed. A. John Wiley & Sons, New York 2001; 487-90.
- Benson AB, Abrams TA, Ben-Josef E, et al. NCCN clinical practice guidelines in oncology: hepatobiliary cancers. J Natl Compr Canc Netw 2009; 7: 350-91.
- Fattovich G, Stroffolini T, Zagni I, Donato F. Hepatocellular carcinoma in cirrhosis: incidence and risk factors. Gastroenterology 2004; 127: 35-50.
- Guo ZS, Thorne SH, Bartlett DL. Oncolytic virotherapy: molecular targets in tumor-selective replication and carrier cell-mediated delivery of oncolytic viruses. Biochim Biophys Acta 2008; 1785: 217-31.
- Bruix J, Sherman M. Management of hepatocellular carcinoma. Hepatology 2005; 42: 1208-36.
- Stahl M, Mariette C, Haustermans K, Cervantes A, Arnold D; ESMO Guidelines Working Group. Oesophageal cancer: ESMO Clinical Practice Guidelines for diagnosis, treatment and follow-up. Ann Oncol 2013; 24 Suppl 6: 51-6.
- Raut RW, Kolekar N, Lakkakula J, Mendhulkar VD. Extracellular synthesis of silver nanoparticles using dried leaves of *Pongamia pinnata* (L) pierre. Nano-Micro Lett 2010; 2: 106.
- Roberson M, Rangari V, Jeelani S, Samuel T, Yates C. Synthesis and characterization silver, zinc oxide and hybrid silver/zinc oxide nanoparticles for antimicrobial applications. Nano Life 2014; 4: 1440003.
- Sumathi S, Dharani B, Sivaprabha J, Raj KS, Padma P. Cell death induced by methanolic extract of *Prosopis cineraria* leaves in MCF-7 breast cancer cell line. Int J Pharmacol Sci Invent 2013; 2: 21-6.
- Azizi M, Ghourchian H, Yazdian F, Dashtestani F, Alizadeh-Zeinabad H. Cytotoxic effect of albumin coated copper nanoparticle on human breast cancer cells of MDA-MB 231. PLoS One 2017; 12: e0188639.
- Chatterjee AK, Sarkar RK, Chattopadhyay AP, Aich P, Chakraborty R, Basu T. A simple robust method for synthesis of metallic copper nanoparticles of high antibacterial potency against *E. coli*. Nanotechnology 2012; 23: 085103.
- El-Sayed IH, Huang X, El-Sayed MA. Selective laser photo-thermal therapy of epithelial carcinoma using anti-EGFR antibody conjugated gold nanoparticles. Cancer Letters 2006; 239: 129-35.
- Chung IM, Abdul Rahuman A, Marimuthu S, et al. Green synthesis of copper nanoparticles using *Eclipta prostrata* leaves extract and their antioxidant and cytotoxic activities. Exp Ther Med 2017; 14: 18-24.
- Chen M, Zhang Y, Huang B, et al. Evaluation of the antitumor activity by Ni nanoparticles with verbascoside. J Nanomaterials 2013; 2013: 623497.
- Rameshthangam P, Pandian Chitra J. Synergistic anticancer effect of green synthesized nickel nanoparticles and quercetin extracted from *Ocimum sanctum* leaf extract. J Mater Sci Technol 2018; 34: 508-22.
- Housein Z, Kareem TS, Salihi A. In vitro anticancer activity of hydrogen sulfide and nitric oxide alongside nickel nanoparticle and novel mutations in their genes in CRC patients. Sci Rep 2021; 11: 2536.
- Al-Snafi A. The chemical constituents and pharmacological effects of *Calendula officinalis* – a review. Indian J Pharm Sci Res 2015; 5: 172-85.
- Ezhilarasi AA, Vijaya JJ, Kaviyarasu K, Maaza M, Ayeshamariam A, Kennedy LJ. Green synthesis of NiO nanoparticles using *Moringa oleifera* extract and their biomedical applications: cytotoxicity effect of nanoparticles against HT-29 cancer cells. J Photochem Photobiol B Biol 2016; 164: 352-60.
- Arulmozhi V, Pandian K, Mirunalini S. Ellagic acid encapsulated chitosan nanoparticles for drug delivery system in human oral cancer cell line (KB). Colloids Surfaces B Biointerfaces 2013; 110: 313-20.

20. Hosseinimehr SJ, Mahmoudzadeh A, Ahmadi A, Ashrafi SA, Shafaghatai N, Hedayati N. The radioprotective effect of *Zataria multiflora* against genotoxicity induced by γ irradiation in human blood lymphocytes. *Cancer Biother Radiopharmaceuticals* 2011; 26: 325-9.
21. Sharmila G, Thirumarimurugan M, Muthukumaran C. Green synthesis of ZnO nanoparticles using *Tecoma castanifolia* leaf extract: characterization and evaluation of its antioxidant, bactericidal and anticancer activities. *Microchem J* 2019; 145: 578-87.
22. Verma PK, Raina R, Agarwal S, Kaur H. Phytochemical ingredients and pharmacological potential of *Calendula officinalis* Linn. *Pharm Biomed Res* 2018; 4: 1-17.
23. Długosz M, Markowski M, Pączkowski C. Source of nitrogen as a factor limiting saponin production by hairy root and suspension cultures of *Calendula officinalis* L. *Acta Physiologiae Plantarum* 2018; 40: 35.
24. de Oliveira Carvalho H, Góes LDM, Cunha NMB, et al. Development and standardization of capsules and tablets containing *Calendula officinalis* L. hydroethanolic extract. *Rev Latinoamericana Química* 2018; 46: 16-27.
25. Sabouri Z, Akbari A, Hosseini HA, Hashemzadeh A, Darroudi M. Eco-friendly biosynthesis of nickel oxide nanoparticles mediated by okra plant extract and investigation of their photocatalytic, magnetic, cytotoxicity, and antibacterial properties. *J Cluster Sci* 2019; 30: 1425-34.
26. Juibari NM, Eslami A. Synthesis of nickel oxide nanorods by *Aloe vera* leaf extract. *J Thermal Analysis Calorimetry* 2019; 136: 913-23.
27. Nwanya AC, Ndingwi MM, Ikpo CO, et al. Zea mays lea silk extract mediated synthesis of nickel oxide nanoparticles as positive electrode material for asymmetric supercapattery. *J Alloys Compounds* 2020; 822: 153581.
28. Ghidan AY, Al-Antary TM, Awwad AM. Green synthesis of copper oxide nanoparticles using *Punica granatum* peels extract: effect on green peach Aphid. *Env Nano-technol Monitoring Manag* 2016; 6: 95-8.
29. Iqbal J, Abbasi BA, Mahmood T, Hameed S, Munir A, Kanwal S. Green synthesis and characterizations of Nickel oxide nanoparticles using leaf extract of *Rhamnus virgata* and their potential biological applications. *Appl Organometal Chem* 2019; 33: e4950.
30. Baranwal K, Dwivedi LM, Singh V. Guar gum mediated synthesis of NiO nanoparticles: an efficient catalyst for reduction of nitroarenes with sodium borohydride. *Int J Biol Macromol* 2018; 120: 2431-41.
31. Rameshthangam P, Chitra JP. Synergistic anticancer effect of green synthesized nickel nanoparticles and quercetin extracted from *Ocimum sanctum* leaf extract. *J Materials Sci Technol* 2018; 34: 508-22.
32. Ibraheem F, Aziz MH, Fatima M, Shaheen F, Ali SM, Huang Q. In vitro cytotoxicity, MMP and ROS activity of green synthesized nickel oxide nanoparticles using extract of *Terminalia chebula* against MCF-7 cells. *Materials Letters* 2019; 234: 129-33.
33. Mahdavi B, Paydarfard S, Zangeneh MM, Goorani S, Seydi N, Zangeneh A. Assessment of antioxidant, cytotoxicity, antibacterial, antifungal, and cutaneous wound healing activities of green synthesized manganese nanoparticles using *Ziziphora clinopodioides* Lam leaves under in vitro and in vivo condition. *Appl Organometal Chem* 2020; 34: e5248.
34. Mahdavi B, Saneei S, Qorbani M, et al. *Ziziphora clinopodioides* Lam leaves aqueous extract mediated synthesis of zinc nanoparticles and their antibacterial, antifungal, cytotoxicity, antioxidant, and cutaneous wound healing properties under in vitro and in vivo conditions. *Appl Organometal Chem* 2019; 33: e5164.
35. Baghayeri M, Mahdavi B, Hosseini-Mohsen Abadi Z, Farhadi S. Green synthesis of silver nanoparticles using water extract of *Salvia leriifolia*: antibacterial studies and applications as catalysts in the electrochemical detection of nitrite. *Appl Organometal Chem* 2018; 32: e4057.
36. Ahmada A, Mahdavi B, Zaker F, et al. Chemical characterization and anti-hemolytic anemia potentials of tin nanoparticles synthesized by a green approach for bioremediation applications. *Appl Organometal Chem* 2020; 34: e5433.
37. Katata-Seru L, Moremedi T, Aremu OS, Bahadur I. Green synthesis of iron nanoparticles using *Moringa oleifera* extracts and their applications: removal of nitrate from water and antibacterial activity against *Escherichia coli*. *J Mol Liq* 2018; 256: 296-304.
38. Radini IA, Hasan N, Malik MA, Khan Z. Biosynthesis of iron nanoparticles using *Trigonella foenum-graecum* seed extract for photocatalytic methyl orange dye degradation and antibacterial applications. *J Photochem Photobiol B Biol* 2018; 183: 154-63.
39. Beheshtkhoo N, Kouhbanani MAJ, Savardashtaki A, Amani AM, Taghizadeh S. Green synthesis of iron oxide nanoparticles by aqueous leaf extract of *Daphne mezereum* as a novel dye removing material. *Appl Phys A* 2018; 124: 363.
40. Sangami S, Manu B. Synthesis of green iron nanoparticles using laterite and their application as a Fenton-like catalyst for the degradation of herbicide Ametryn in water. *Environm Technol Innov* 2017; 8: 150-63.